Journal of Materials Chemistry B

Accepted Manuscript

ROYAL SOCIETY OF CHEMISTRY

www.rsc.org/materialsB

Cite this: DOI: 10.1039/c0xx00000x

www.rsc.org/xxxxxx

ARTICLE TYPE

Preparation of Porous Cellulose 3,5-Dimethylphenylcarbamate Hybrid Organosilica Particles for Chromatographic Applications

Xilun Weng[a], Zongbi Bao[a]*, Zhiguo Zhang[a], Baogen Su[a], Huabin Xing[a], Qiwei Yang[a], Yiwen Yang[a], and Qilong Ren[a]

Received (in XXX, XXX) XthXXXXXXXXX 20XX, Accepted Xth XXXXXXXXX 20XX
DOI: 10.1039/b000000x

Abstract: Organic-inorganic hybrids incorporating cellulose tris(3,5-dimethylphenylcarbamate) (CDMPC)-functionalized silica particles can exhibit high loading capacity with high loadings of the chiral selector. These materials offer considerable potential for use in preparative chiral separations. However, the preparation of these hybrid particles with high surface areas and controlled organic/inorganic ratios is challenging. We have found that by controlling the pH of sol-gel step and regulating the ratio of the inorganic precursor over CDMPC, unique functional hybrid particles could be prepared with optimum pore structure, novel interfacial features and excellent mechanical strength. The morphological features of these hybrid particles were characterized by scanning electron microscopy (SEM) and transmission electron microscopy (TEM). The organic content was determined by thermogravimetric analysis (TGA) and pore structure determined by Brunauer, Emmett and Teller (BET) analysis. These new hybrid particles exhibit excellent solvent durability which is crucial for preparative chromatography. HPLC analysis of columns packed with this material confirmed solvent tolerance such as chloroform, giving potential applications for large scale chromatographic separations.

1 Introduction

Organic-inorganic hybrid materials offer a wide range of multifunctional properties for applications in electronics, optics, biochemistry and medicine.[1-4] Recently hybrid organosilica spheres with a uniform spherical shape and narrow pore size distribution (PSD) have attracted considerable attention as HPLC packing materials in part because of their high mechanical strength and chemical stability.[5-8] With control of the organic-inorganic ratio, these hybrid organosilica spheres are able to satisfy the requirements for an ideal HPLC packing to achieve a high density of functional groups and high column efficiency.[9]

Enantioselective chromatography with chiral stationary phases (CSPs) is recognized as a practical method for obtaining optically pure enantiomers. Polysaccharides and their related derivatives with high chiral helical contents make ideal raw materials for HPLC packing. A number of commercial CSPs that utilize polysaccharide based CSPs developed by Okamoto group have broad recognition ability and high column capacity.[10, 11] Therein, cellulose tris(3,5-dimethylphenylcarbamate) (CDMPC) exhibits universal chiral discrimination for racemates.[12-14] Up to now, commercial chiral packing materials are generally prepared by coating or immobilizing chiral selectors on a macroporous silica gel support. This limits the column capacity because the chiral selector density is usually below 20 wt% upon silica.[15] To improve the loading capacity of cellulose CSPs, the Okamoto group reported spherical CDMPC beads with a high loading capacity but poor mechanical strength.[16, 17] In 2008, the same group reported the synthesis of silica-based CDMPC hybrid particles for enantioseparation by HPLC with the CDMPC content up to 70 wt%.[18] Importantly, the material also has excellent mechanical strength. These CDMPC hybrid beads have advantages such as higher loading capacity over currently used column packing materials in commercial chiral columns.

However when CDMPC hybrid beads are used as chromatographic supports, it swells intensively or even becomes partially soluble in solvents such as chloroform and THF.[18] A gradual elevation of column pressure was observed when the cellulose derivative content reaches 70%,[15, 18] which might result from high organic ratio of hybrid particles. For preparative column chromatography, the resolution efficiency and loading capacity depend on the solubility (or concentration) of racemates in the eluent. The solubility of many commercial drugs in mobile phases such as hexane and isopropanol is poor, but is good in solvents containing chloroform. For example, the solubility of racemates such as *N*-(1-naphthyl)ethyl-4-nitrobenzamide can be increased by a factor of 300–500 with chloroform as the mobile phase.[19]

Based on the pioneering work of Stober[20] and Unger[21] for the synthes is of silica particles with control of porosity and morphology, sol−gel chemistry provides a convenient route to chemically homogeneous organic/inorganic hybrid network

Cite this: DOI: 10.1039/c0xx00000x

www.rsc.org/xxxxxx

ARTICLE TYPE

materials with uniformity of physical properties and high surface area.[20-22] However, due to the immiscibility between hydrophobic cellulose derivatives and hydrophilic silica framework, the synthesis of cellulose derived hybrid particles with high surface area and controlled organic/inorganic ratio via sol-gel chemistry is challenging. Shea and coworkers reported conditions used for synthesis of organic-bridged polysilsesquioxane xerogels with high surface area that is confined to the micropore and mesopore domain.[23] Their conditions are useful for the preparation of hybrid CDMPC-Si particles with pH sensitive properties.

To solve the swelling issues of silica-based CDMPC hybrid particles, we focus on the regulation of its organic-inorganic content. In this article, we report the preparation of mesoporous organosilica spheres containing a CDMPC-based selector with porous structure, unique interfacial properties and excellent mechanical strength. Their use as a chiral stationary phase with excellent chiral discrimination ability and solvent durability to chloroform was confirmed.

2 Experimental

2.1 Materials

Microcrystalline cellulose (Avicel, DP-200) was acquired from FMC Biopolymer. 3,5-Dimethylphenyl isocyanate (99%) and tetraethoxysilane (98%) were obtained from Sigma-Aldrich. 3-(Triethoxysilyl)propyl isocyanate (95%), trimethylsilyl chloride (TMSCl) (98%), lithium chloride (AR), and 1-heptanol (99%) were provided by Aladdin Reagent Co. (Shanghai, China). Racemic 2,2,2-trifluoro-1-(9-anthryl)ethanol (>99%) was purchased from TCI, and pindolol (99.5%) was supplied by J&K (Shanghai, China). HPLC-grade n-hexane and isopropanol were obtained from TEDIA. Analytical-grade methanol, ethanol, n-propanol, chloroform, tetrahydrofuran and pyridine were obtained from Sinopharm (Beijing, China). Diethylamine (≥99.0%) was purchased from Wulian Shanghai Reagent Co. (China). 1,3,5-Tri-tert-butylbenzene (97%) as non-retained compound for HPLC was provided by Sigma-Aldrich. Sodium dodecyl sulfate (SDS) was bought from Xilong chemical engineering company (China).

2.2 Synthetic procedures

2.2.1 Preparation of CDMPC monomer bearing 3-(triethoxysilyl)propyl groups

The CDMPC bearing 3-(triethoxysilyl)propyl groups (denoted as CDMPC-Si monomer) was prepared according to a previously reported method.[24] The reaction was carried out in nitrogen atmosphere. Cellulose (1.0 g) was dissolved in a mixture of dry *N*,*N*-dimethylacetamide (40 mL), anhydrous lithium chloride (4.0 g) and anhydrous pyridine (20 mL). Then 2.1 g of 3,5-dimethylphenyl isocyanate was added and the mixture was stirred for 8 h at 80 °C. Subsequently a known amount (0.33 g or 3.3 g) of 3-(triethoxysilyl)propyl isocyanate was added and the mixture continued to react for an extra 12 h at 80 °C. Finally, an excess amount of 3,5-dimethylphenyl isocyanate (3.2 g) was added to derivatize all residual hydroxyl groups on the cellulose backbone for another 8 h at the same temperature (Scheme 1 step 1). At the end of the 28 h reaction, the obtained brown sticky liquid was poured into 150 mL methanol and white precipitate was observed. This insoluble fraction was washed several times with methanol and dried under vacuum to give CDMPC-Si monomer (Table 1). Structure of CDMPC-Si monomer was identified by ^{1}H NMR (Figure S1).

2.2.2 Preparation of hybrid CDMPC-based silica particles

In a typical synthesis of hybrid CDMPC-based silica particles, CDMPC-Si monomer (0.25 g) was dissolved in the mixture of THF/1-heptanol/H_2O (32 mL/6 mL/1 mL). Various amounts of TMSCl were added (Table 1), which was then heated at 80°C for 15 h (Scheme 1 step 2). After the sol-gel reaction went to completion, the obtained mixture was poured into the aqueous solution containing SDS (500 mL, 0.2 wt%) of different pH (2, 7 or 9) at 80 °C with mechanical stirring at 1100 rpm (Scheme 1 step 3). After filtration, the sample was washed thoroughly with hot aqueous ethanol followed by n-hexane at room temperature. Structures of cellulose, CDMPC-Si monomer and hybrid CDMPC silica spheres were identified by IR spectrum (Figure S2). Structure of hybrid CDMPC silica spheres was identified by Solid ^{13}C NMR (Figure S3).

The obtained hybrid CDMPC silica materials (1.0 g) were further treated via an end-capping process by refluxing in dry toluene (20 mL) and TMSCl (10 mL) for 8 h under nitrogen atmosphere.[25] After filtration, the product was washed with toluene and methanol, and then dried in vacuum at 60 °C.

2.2.3 Packing of hybrid CDMPC-based silica particles column

The hybrid chiral stationary phase was packed by using a stainless-steel column (150 mm × 4.6 mm I.D.) at a pressure of 400 kg/cm^2 by a slurry method with n-hexane and isopropanol (90:10, v/v).

2.3 Characterization

^{1}H NMR spectrum of CDMPC-Si was acquired in acetone-d_6 at 200 MHz on a DMX-500 NMR Spectrometer (BRULCER CO. (SP)). A Micromeritics ASAP 2050 adsorption apparatus was used to measure the N_2 adsorption isotherms at 77 K. Brunauer-Emmett-Teller (BET) specific surface area was calculated from N_2 adsorption isotherm at 77 K in the relative pressure range of 0.05~0.30 after 80 ^{o}C degas treatment for 15 h (All samples were dried in the vacuum for 15 h at 80 ^{o}C before degas). PSD was obtained from the N_2 desorption branch at 77K using the Nonlocal density function theory (NLDFT) method. Transmission electron microscopy (TEM) image was observed by a Titan ChemiSTEM (FEI) at an acceleration voltage of 200 kV. Scanning electron microscopy (SEM) image was undertaken on a

Cite this: DOI: 10.1039/c0xx00000x

www.rsc.org/xxxxxx

ARTICLE TYPE

SIRON scanning electron microscope (FEI) operating at an accelerating voltage of 25 kV. The thermogravimetric analysis (TGA) was measured on a Pyris 1 TGA instrument (PerkinElmer) at a heating rate of 10 °C/min under air flow. Chromatographic separation was performed on a Waters HPLC system (Milford, MA, USA), equipped with a 1525 binary HPLC pump, a Waters 717 plus auto-injector and a Waters 2487 dual λ absorbance UV detector. The analysis was carried out at 30 °C with injection volume of 10 µL. The determination of the particle size distribution was performed with a LS particle size analyzer (Beckman Coulter LS 13320, USA) at room temperature with an equilibrium time of 90 s. The solid-state ^{29}Si CP/MAS NMR spectrum and ^{13}C CP/MAS NMR spectrum were recorded on a 400 MHz WB solid-state NMR Spectrometer and a Bruker AVANCE III 400 MHz (Switzerland).

Table 1. TGA and S_{BET} characterization of the hybrid materials synthesized under different sol-gel conditions.

Sample[a]	Dimethylphenyl/3-(triethoxysilyl)propyl	Amount of TMSCl (uL)	pH of aging	Cross-linking time (h)	Inorganic content (%)	S_{BET} (m^2/g)	$D_p^{DFT\,b}$ (nm)	V_p^{DFTc} (cm^3/g)
HL-15-2	98:2	500	2	15	~20	<10	–	–
HL-15-7	98:2	2	7	15	~0	<10	–	–
HH-15-2	90:10	500	2	15	~35	43.4	–	0.02
HH-15-9	90:10	2	9	15	~50	217.9	9.9	0.38
HH-15-7	90:10	2	7	15	~50	522.4	4.0	0.45
HH-13-7	90:10	2	7	13	~50	396.6	6.1	0.41
HH-11-7	90:10	2	7	11	~50	276.8	9.7	0.44
HH-9-7	90:10	2	7	9	~50	247.0	13.8	0.41

[a] HL stands for hybrid materials synthesized from CDMPC with low ratio of dimethylphenyl/3-(triethoxysilyl)propyl (98:2), HH stands for hybrid materials synthesized from CDMPC with high ratio of 3-(triethoxysilyl)propyl/dimethylphenyl (90:10) [b] Vp^{DFT} is the total pore volume determined by the NLDFT method. [c] D_p^{DFT} is the pore diameter determined by the NLDFT method.

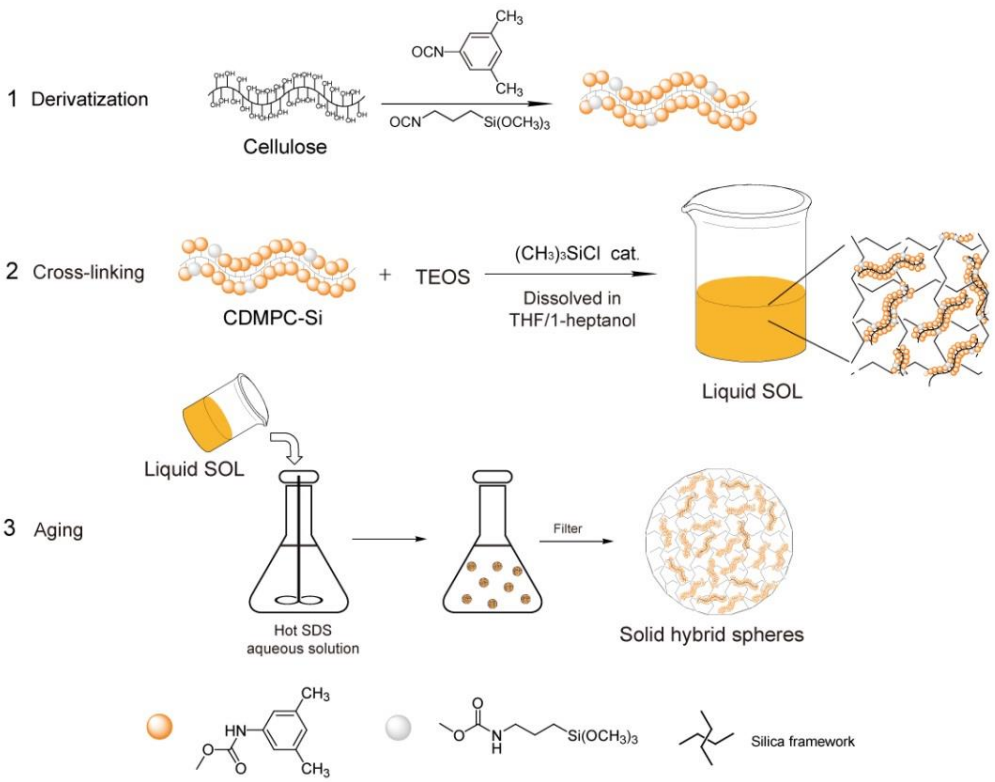

Scheme 1 Schematic of the process to prepare hybrid CDMPC silica spheres.

Cite this: DOI: 10.1039/c0xx00000x

www.rsc.org/xxxxxx

ARTICLE TYPE

3 Results and discussion

Sol-gel process formation study

The preparation of CDMPC-functionalized silica particles was accomplished in three steps (Scheme 1): **1. Derivatization of cellulose to CDMPC-Si monomer:** the hydroxyl groups of cellulose were derivatized as CDMPC with various ratios of 3,5-dimethylphenyl isocyanate over 3-(triethoxysilyl)propyl isocyanate (Table 1); **2. Cross-linking of CDMPC-Si monomer and TEOS:** CDMPC-Si was dissolved in the mixture of THF and 1-heptanol and then mixed with TEOS. Water and TMSCl were used as catalysts to form a sol; **3. Aging:** the sol was poured into a hot aqueous solution containing SDS with vigorous stirring to form solid spherical particles.

We regulated the sol-gel process in making hybrid CDMPC-based silica particles in two aspects: 1. Control of the amount of TMSCl in the cross-linking step, which not only affects the final inorganic content of hybrid CDMPC particles but also influences the pH of the system (Scheme 1, step 2). 2. Control of pH in the aging step (Scheme 1, step 3) which can affect the final porosity and morphology of the particles.

Before regulating the sol-gel condition, control of the ratio of 3-(triethoxysilyl)propyl content over 3,5-dimethylphenyl-carbamate content in the derivatization step is important (Scheme 1, step 1). When the 3-(triethoxysilyl)propyl content is 2% (Table 1, HL-type CDMPC-Si), cross-linking between CDMPC-Si monomer and TEOS only occurs under strong acidic conditions (Table 1, sample HL-15-2). Under neutral cross-linking conditions (Table 1, sample HL-15-7), we only observed pure CDMPC-Si irregular shaped particles after aging (Figure S4). From TGA analysis, sample HL-15-2 has 20% inorganic residue while sample HL-15-7 has no residue (Table 1). These results suggest that the organic-inorganic cross-linking does not occur under neutral sol-gel conditions when the (triethoxysilyl)propyl content is only 2%. This is probably due to low degree of cross-linking between HL-type CDMPC-Si monomer and the silica precursor under slightly acidic conditions. When the amount of 3-(triethoxysilyl)propyl groups was increased to 10 % (Table 1, HH-type CDMPC-Si), formation of hybrid materials and regulation of the inorganic content is possible under neutral conditions.

The amount of TMSCl is crucial in regulating the inorganic ratio of hybrid particles. In addition to act as an acidic catalyst, TMSCl can function as an end-capping agent to terminate the polycondensation reaction (Scheme 2). Therefore, relatively small amount of TMSCl is more likely to increase the inorganic content of hybrid beads. From TGA analysis, HH-15-7 and HH-15-9 with a lower amount of TMSCl exhibit a much higher residue (50%) than that of HH-15-2 (35%) (Table 1, Figure 1). Occurrence of the end-capping reaction can be supported by ^{29}Si MAS NMR analysis that sample HL-15-2 has a clear $Si(CH_3)_3$ peak which is not observed in the sample HH-15-7 (Figure2). On the other hand, both sample HH-15-7 and HL-15-2 show Si-O-Si bonds which could be confirmed by a single broad peak centered at -100 ppm (Q^3(Si(OH or OEt)$(OSi)_3$)) together with two shoulders at -90 ppm (Q^2(Si(OH or OEt)$_2(OSi)_2$)) and -110 ppm (Q^4(Si$(OSi)_4$)) (Figure 2, line b). However, the existence of Q^2 and Q^3 indicates that the polycondensation of TEOS did not proceed to completion and the silanol or ethoxysilyl groups remained in both samples. Compared with HL-15-2 from our previous work,[15] sample HH-15-7 exhibits a higher particle size (Figure 3), which was treated with a lower concentration of TMSCl. The mean particle diameter of HH-15-7 is 17.3 μm, higher than 12.0 μm from sample HL-15-2 (Figure 3). This also proves that use of TMSCl halts the growth of the Si-O-Si chains and promotes the end-capping of the particles which could lead to a smaller particle size.

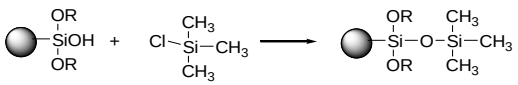

Scheme 2 End-capping reaction with TMSCl.

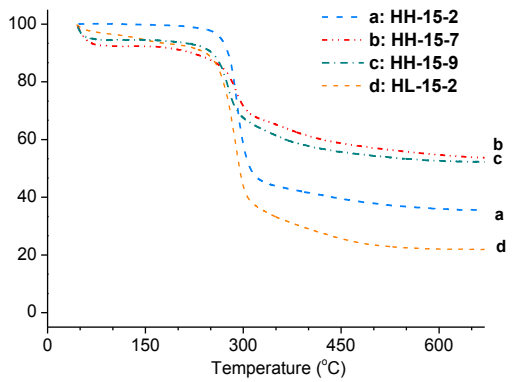

Figure 1 Thermogravimetric analysis of hybrid materials prepared under different sol-gel conditions

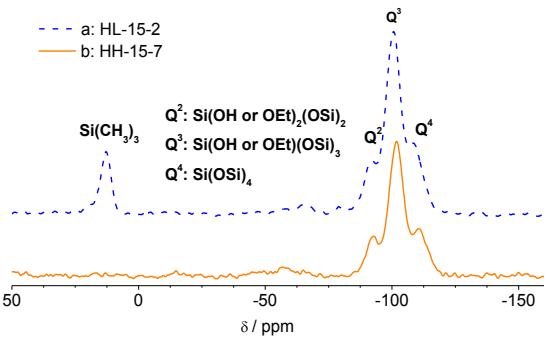

Figure 2 Solid-state ^{29}Si CP/MAS NMR spectrum of a: HL-15-2, b: HH-15-7.

Cite this: DOI: 10.1039/c0xx00000x

www.rsc.org/xxxxxx

ARTICLE TYPE

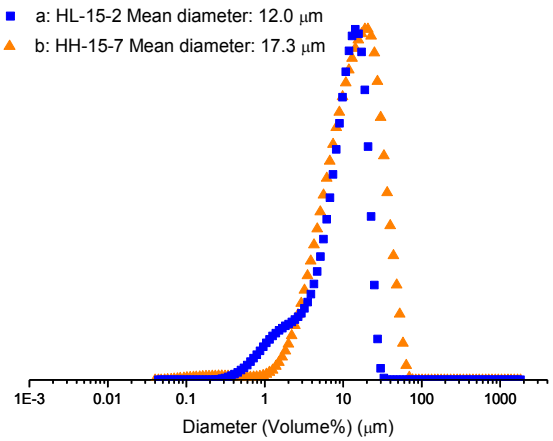

Figure 3 Particle size distribution of sample a: HL-15-2, b: HH-15-7.

Controlled surface morphology of silica-based CDMPC hybrid particles

We chose three samples to demonstrate this interesting phenomenon with SEM (Figure 4). The surface of the hybrid beads exhibits a transition from smooth to rough with an increasing amount of the inorganic content and increasing pH during the aging process.

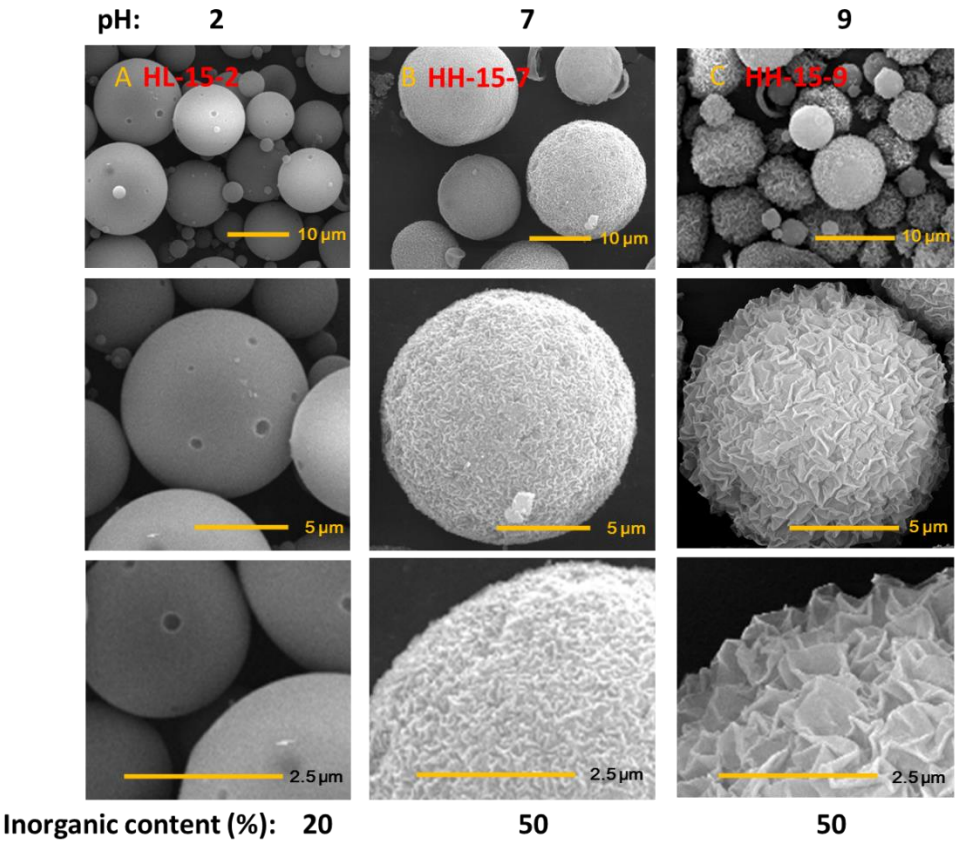

Figure 4 SEM micrographs of particles prepared under different sol-gel conditions* (A, B, C)

*Preparation of sol-gel condition is listed in Table 1.

Cite this: DOI: 10.1039/c0xx00000x

www.rsc.org/xxxxxx

ARTICLE TYPE

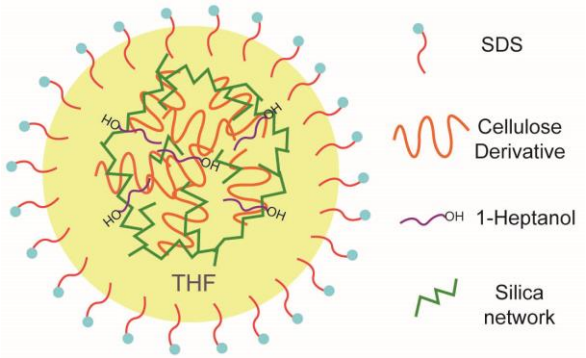

Figure 5 Depiction of a possible constitution of hybrid spheres in the aging process.

A schematic of hybrid spheres constituted during the aging process is given in Figure 5 to describe the possible mechanism of this interfacial phenomenon. To prepare the sol, CDMPC was fully dissolved in THF/1-heptanol and cross-linked with TEOS for 15 h at 80 °C (Scheme 1, step 2). Co-condensation reaction occurs between hydrophobic CDMPC-Si monomer and hydrophilic TEOS. The ratio of organic and inorganic components is crucial for controlling the morphology of hybrid particles during aging because of their different hydrophobic lipophilic balance (HLB) properties. Since the inorganic content undergoes an apparent change when varying the amount of TMSCl during cross-linking, the change of the HLB property of the particles would cause an interfacial instability and lead to a controlled surface morphology. When the particles were dispersed in the aqueous SDS solution and aged, interfacial equilibrium of hybrid spheres with 20% inorganic content remained stable and formed smooth spheres (Figure 4A). However, with the extension of the silica chain and elevation of the inorganic content, the particles became more hydrophilic. The original interfacial balance is about to be broken. When interfacial excess continues to increase, the imbalance finally triggers the original surface at the interface from smooth to rough (Figure 4B) to reach interfacial equilibrium.[26] A similar process of interfacial roughening and droplet ejection have been reported for oil–water amphiphile systems.[27]

On the other hand, sample HH-15-9 has almost the same inorganic content with HH-15-7 (Table 1), but it exhibits a more wrinkled surface. This indicates that different aging pH is also important to influence the interfacial instability of CDMPC-silica system and thus change the surface morphology. It is common that electrostatic interactions between the oppositely charged surfactants would contribute to interfacial instability. During aging, anionic surfactant SDS facilitates to stabilize surface of hybrid spheres. When aging pH was increased to 7 or even 9 inorganic silica chain would be negatively charged. The repulsion between inorganic silica and the anionic surfactant SDS would lead to a gradual increase in interfacial instability and finally cause collapse of spherical morphology (Figure 4B, C).[28]

pH and reaction time dependent BET surface area and pore structure of CDMPC hybrid particles

Many polymer based spherical materials are nonporous due to the collapse of soft polymer chains.[26] However in a typical sol-gel system involving large hydrophobic organic groups such as CDMPC, the final porosity is extremely pH sensitive. For,

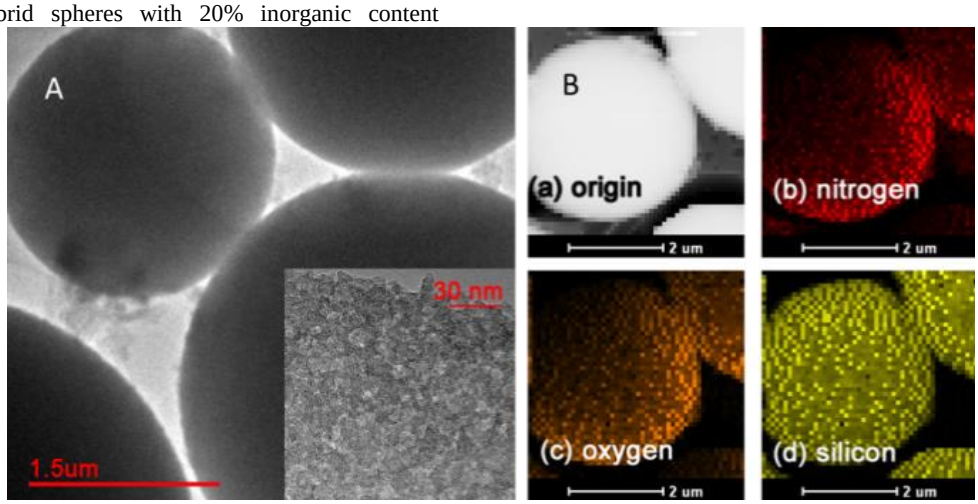

Figure 6 TEM image of the synthesized HH-15-7 (A) and energy-dispersive X-ray (EDX) mapping patterns of origin (a), nitrogen (b), oxygen (c), silicon (d) of HH-15-7 (B).

Cite this: DOI: 10.1039/c0xx00000x

www.rsc.org/xxxxxx

ARTICLE TYPE

example, HH-15-2 prepared under acidic aging conditions exhibits very low surface area. Mesoporous structure and high BET surface area was found when neutral or basic conditions were employed (Table 1, HH-15-7 and HH-15-9). Analysis of TEM and energy dispersive X-ray (EDX) confirms formation of a porous structure (Figure 6A) and uniformly distributed chemical composition of HH-15-7 (Figure 6B). pH is a key factor to obtain porous hybrid silica particles. With the same cross-linking time, hybrid particles synthesized under neutral aging conditions resulted in the highest BET surface area (Table 1, HH-15-2, HH-15-7 and HH-15-9). It is interesting that the material exhibits similar properties as alkylene-bridged polysilsesquioxane reported by Shea and coworkers.[23] Polycondensation of monomers bearing more flexible bridging groups under acidic conditions results in non-porous gels.[29-31] When the aging condition becomes basic, the BET surface area decreases from 522.4 m^2/g to 217.9 m^2/g with the extension of pore size from 40 Å to 99 Å (Table 1, HH-15-7, HH-15-9). It indicates that the porosity depends on the pH of both cross-linking and aging steps. In neutral or basic solutions, the gel porosity is remarkably coarsened by alkalis as an aging promoter. Unlike using strong acids in the aging step (pH<2), alkalis can dissolve the gel under basic conditions. Therefore the pore size can be enlarged by partially dissolution of the silica. Aging in a neutral or basic solution results in a one-way process: loss of specific surface area and increase in pore size.[32] A similar mechanism has also been proved on the classical sol-gel reaction.[33, 34]

Most macroporous silica columns coated with polysaccharide derivatives have relatively low surface area. For example, the BET surface area is often reduced to 20 m^2/g following polysaccharide derivatization via coating or surface immobilization. A significant finding of the present work is that for the first time we were able to develop polysaccharide hybrid packing materials with comparatively high surface area and mesoporous structure. This combination of properties can offer certain advantages for chiral separations.

The collapse of porosity during CDMPC-Si aging does not occur under neutral or basic conditions, suggesting that there may be a kinetic contribution to create porosity in addition to the network compliance model. The hydrolysis and condensation of the precursors require time to achieve equilibrium, and porous structure of CDMPC-Si hybrid particles might vary depending on the time allotted for the sol step. To learn if this variable contributes to the observed morphology we investigated the effect of cross-linking time for the sol step on the porous structure of final products. Figure 7 shows the N_2 adsorption–desorption isotherms for the synthesized materials. HH-9-7, HH-11-7, HH-13-7 and HH-15-7 materials show type IV nitrogen adsorption–desorption curve, according to the IUPAC classification, which are typical of porous solids. The steep adsorption step detected around p/p_0 = 0.4–1.0, corresponding to the capillary condensation of nitrogen, also evidences the formation of porous structured solid materials. Samples HH-9-7, HH-11-7 and HH-13-7 exhibit type H2 hysteresis loop which indicates an interconnected system in pores with narrow necks and wide bodies (often referred to as 'ink bottle' pores). However, HH-15-7 is more likely to be H4 type which appear to be associated with narrow slit-like pores.[35] Samples HH-9-7, HH-11-7 and HH-13-7 in Figure 7 exhibit a forced closure due to a sudden drop in the volume adsorbed along the desorption branch in the p/p_0 around 0.5, which is often denoted as Tensile Strength Effect (TSE).[36] We chose NLDFT model to calculate PSD rather than using BJH model due to the existence of TSE phenomenon in the desorption branch.[36] As the cross-linking time increased from 9 to 15 h, the BET surface area increased from 247.0 m^2/g to 522.4 m^2/g, while the pore size decreases from 138 Å to 40 Å (Table 1, HH-9-7, HH-11-7, HH-13-7 and HH-15-7). The pore volume of these samples, however, remains constant at approximately 0.4 cm^3/g (Table 1). The morphology change of pore structure as a function of the cross-linking time is interpreted by both transition of hysteresis loops and PSD analysis. We conclude that the porous features of the materials can be controlled by the length of cross-linking time, which is related to the kinetics of hydrolysis and condensation.

Cite this: DOI: 10.1039/c0xx00000x

www.rsc.org/xxxxxx

ARTICLE TYPE

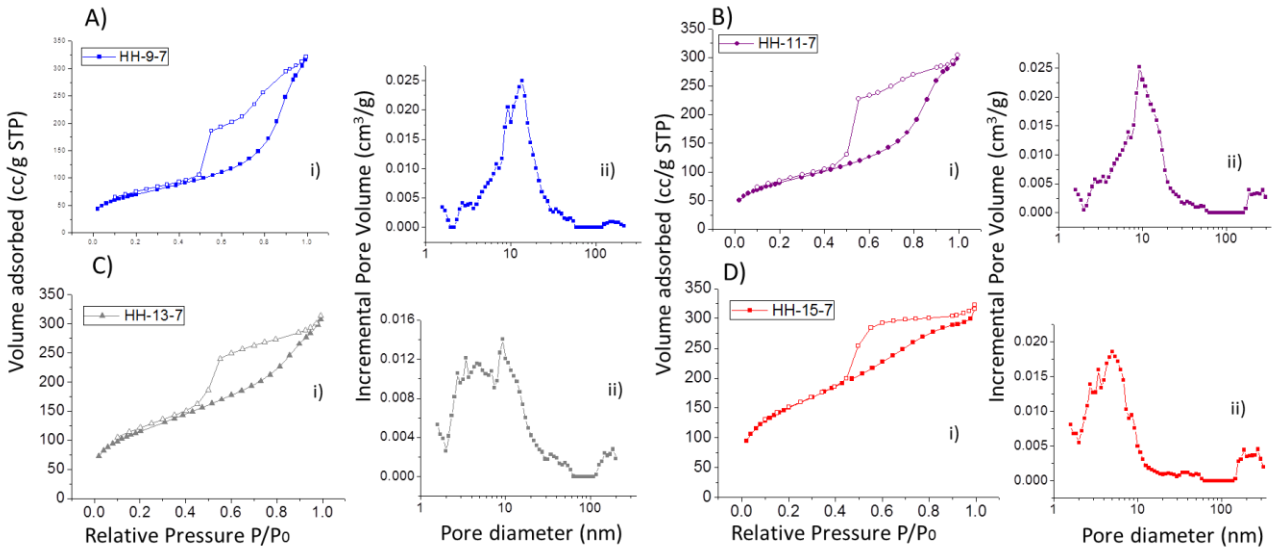

Figure 7 Nitrogen adsorption/desorption isotherms and pore size distribution of HH-9-7 (A), HH-11-7 (B), HH-13-7 (C), HH-15-7 (D)

Chromatographic evaluation

The utility of these materials as HPLC stationary phases require mechanical strength and the ability to discriminate chiral structures. HL-15-2 has already been carefully studied as HPLC packing materials for resolution of some standard racemates and beta-blockers.[15] Based on a number of criteria including good spherical morphology, high surface area of 522.4 m^2/g and narrow pore size of 40 Å, HH-15-7 was selected to be an ideal HPLC packing material. Moreover, its high inorganic content is expected to increase the rigidity of packing material; and chiral selector density which is higher compared to the coating and immobilizing of commercial columns (20%). In order to test its performance as HPLC support, the material was packed into a 150 mm × 4.6 mm I.D. column.

It is noteworthy that the HH-15-7 packing material is of great mechanical strength (Figure 8, line b). Significant lower column pressure was observed when using HH-15-7 as the packing material compared to the one using HL-15-2. Figure 8 also indicates an excellent linearity with flow rate up to 2 mL/min when running the column in HPLC. The apparent low column pressure of the HH-15-7 column could also be attributed to the reduced deformation under high column pressure as well as the existence of mesoporous structure which improves the permeability.

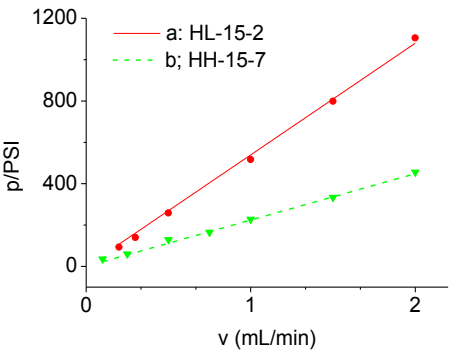

Figure 8 Relationship of volumetric flow-rate (x axis) and pressure drop across the columns (y axis) packed of a) HL-15-2 and b) HH-15-7. Line a was acquired from our previous work.[15]

Cite this: DOI: 10.1039/c0xx00000x

www.rsc.org/xxxxxx

ARTICLE TYPE

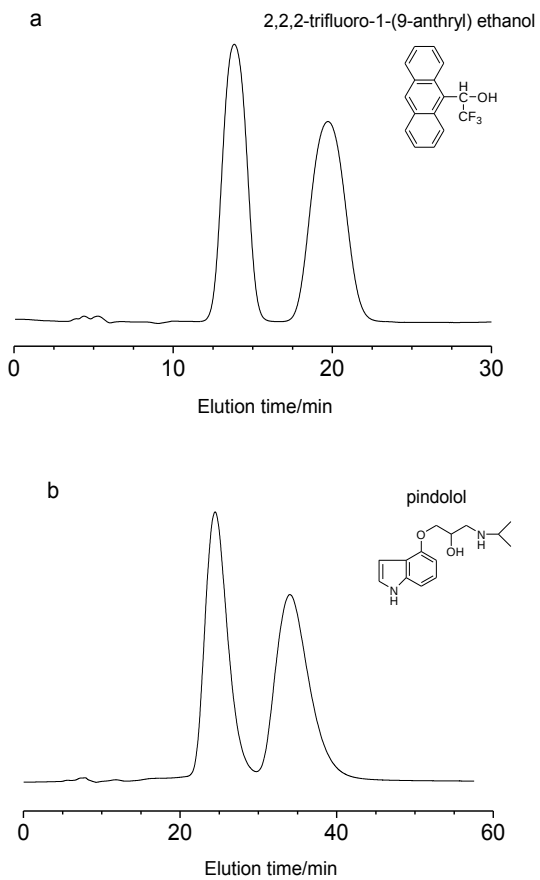

Figure 9 Chromatograms for the resolution of 2,2,2-trifluoro-1-(9-anthryl) ethanol (A) and pindolol (B)

After end-capping treatment to eliminate the potential negative effect of surface silanols, the column was evaluated on a Waters HPLC system to test its chiral discrimination ability using racemic 2,2,2-trifluoro-1-(9-anthryl)ethanol enantiomers as the probe. Figure 9 shows the chromatograms of two racemic enantiomers including 2,2,2-trifluoro-1-(9-anthryl)ethanol and pindolol using n-hexane/ethanol (95:5, v/v) and n-hexane/chloroform/ethanol/diethylamine (75:10:15:0.5, v/v/v/v) as mobile phases, respectively. As shown in Figure 9a, the resolution of 2,2,2-trifluoro-1-(9-anthryl)ethanol achieves baseline separation with symmetrical peaks. The retention factor of less retained enantiomer (k_1') is 2.58 with the selectivity α of 1.6. Compared to the α value of 1.91 by Okamoto etc.,[18] the hybrid CSP spheres possess slightly lower chiral recognition ability. Because the chiral discrimination ability is mainly influenced by a single chiral selector like CDMPC, elevation of 3-(triethoxysilyl)propyl groups on the backbone would inevitably destroy its helical structure and lower the chiral recognition ability.

With the change of chemical compositions of this hybrid particle, its durability toward solvents such as chloroform is improved. The HH-15-7 column was flushed by n-hexane/chloroform/ethanol (85:10:5, v/v/v) for at least 12 h, and the pressure across the column remained unchanged with stable enantioseparation ability, proving its excellent anti-swelling ability. As mentioned in Okamoto's work[18] and also confirmed by us, HL-15-2 is not tolerant to eluents containing a high volume percent of solvents such as chloroform or THF, since its high organic content might lead to swelling or even partial dissolution which gradually elevating the column pressure.[18] This property is a serious drawback in enantioseparation on a preparative scale such as Simulated Moving Bed (SMB) separation. In some cases, addition of solvents including dichloromethane and chloroform into the mobile phase is beneficial for productivity in practical preparative chiral chromatography, for they can improve the solubility of the feedstock in the mobile phase. Pindolol, a typical β-adrenergic blocking agent, can be resolved by Chiralcel OD column but the compound has very limited solubility in the mobile phase (n-hexane/isopropanol or ethanol). In our case, however, pindolol is baseline resolved with the existence of chloroform. As shown in Figure 9b, a satisfactory result with acceptable retention factor of 2.9 and enantioselectivity of 1.5 could be obtained using eluent containing 10% chloroform in the n-hexane/ethanol/diethylamine solvent mixture. In this case, the solubility of pindolol in the mobile phase could be elevated by several orders of magnitude compared to that without chloroform. This feature is beneficial for applications on preparative columns.

4 Conclusions

Sol–gel processed mesoporous CDMPC organosilica hybrid particles were prepared under a variety of reaction conditions. The systematic variation of differences in cross-linking time, pH of sol-gel and inorganic content were performed to lead to novel interfacial features of the resulting hybrid materials. The porosity of the resulting particles was shown to exhibit the same dependence on the pH of the sol–gel polymerizations. The combination of high surface area, pore size and inorganic content led to a new chromatographic material with a combination of desirable properties for enantiomer resolution. Baseline separation of racemic 2,2,2-trifluoro-1-(9-anthryl) ethanol were achieved and eluent durability of column packed with HH-15-7 was confirmed. β-Blocker, e.g. pindolol has also been successfully resolved using eluents containing chloroform, which indicates the packing material has potential use in preparative chiral chromatographic separation.

Acknowledgements

Cite this: DOI: 10.1039/c0xx00000x

www.rsc.org/xxxxxx

ARTICLE TYPE

The authors are grateful for the financial support from the National Natural Science Foundation of China (No. 21376205 and No.21222601) and Zhejiang Provincial Natural Science Foundation of China (No. Y13B060004).

Notes and references

[a]*Key Laboratory of Biomass Chemical Engineering of Ministry of Education, Department of Chemical and Biological Engineering, Zhejiang University, Hangzhou 310027, China*
E-mail:baozb@zju.edu.cn

† Electronic Supplementary Information (ESI) available: [details of any supplementary information available should be included here]. See DOI: 10.1039/b000000x/

1 C. Sanchez and F. Ribot, *New J. Chem.*, 1994, **18**, 1007-1047.
2 G. Schottner, *Chem. Mater.*, 2001, **13**, 3422-3435.
3 D. Avnir, T. Coradin, O. Lev and J. Livage, *J. Mater. Chem.*, 2006, **16**, 1013-1030.
4 A. Fidalgo, R. Ciriminna, L. M. Ilharco and M. Pagliaro, *Chem. Mater.*, 2005, **17**, 6686-6694.
5 V. Rebbin, R. Schmidt and M. Fröba, *Angew. Chem.-Int. Edit.*, 2006, **45**, 5210-5214.
6 S. Chen, S. Hayakawa, Y. Shirosaki, E. Fujii, K. Kawabata, K. Tsuru and A. Osaka, *J. Am. Chem. Soc.*, 2009, **92**, 2074-2082.
7 S. Inagaki, S. Guan, Q. Yang, M. P. Kapoor and T. Shimada, *Chem. Commun.*, 2008, 202-204.
8 M. Benitez, G. Bringmann, M. Dreyer, H. Garcia, H. Ihmels, M. Waidelich and K. Wissel, *J. Org. Chem.*, 2005, **70**, 2315-2321.
9 M. C. Frank Hoffmann, J. Morell, and M. Fröba, *Angew. Chem. Int. Ed.*, 2006, **45**, 3216 – 3251.
10 T. Ikai and Y. Okamoto, *Chem. Rev.*, 2009, **109**, 6077-6101.
11 T. Ikai, C. Yamamoto, M. Kamigaito and Y. Okamoto, *Chem. Rec.*, 2007, **7**, 91-103.
12 Y. Okamoto and Y. Kaida, *J. Chromatogr. A*, 1994, **666**, 403-419.
13 E. Yashima, *J. Chromatogr. A*, 2001, **906**, 105-125.
14 Y. Okamoto and T. Ikai, *Chem. Soc. Rev.*, 2008, **37**, 2593-2608.
15 X. Weng, Z. Bao, H. Xing, Z. Zhang, Q. Yang, B. Su, Y. Yang and Q. Ren, *J. Chromatogr. A*, 2013, **1321**, 38-47.
16 T. Ikai, R. Muraki, C. Yamamoto, M. Kamigaito and Y. Okamoto, *Chem. Lett.*, 2004, **33**, 1188-1189.
17 T. Ikai, C. Yamamoto, M. Kamigaito and Y. Okamoto, *J. Sep. Sci.*, 2007, **30**, 971-978.
18 T. Ikai, C. Yamamoto, M. Kamigaito and Y. Okamoto, *Chem. Asian J.*, 2008, **3**, 1494-1499.
19 E. R. Francotte, *J. Chromatogr. A*, 2001, **906**, 379-397.
20 W. StÔber, A. Fink and E. Bohn, *J. Colloid Interface Sci.*, 1968, **26**, 62-69.
21 K. Unger, J. Schick-Kalb and K.-F. Krebs, *J. Chromatogr. A*, 1973, **83**, 5-9.
22 J. Wen and G. L. Wilkes, *Chem. Mater*, 1996, **8**, 1667-1681.
23 K. Shea, J. Moreau, D. Loy, R. Corriu and B. Boury, *Functional Hybrid Materials*, eds. P. G. Romero and C, Sanchez, Wiley 2004, pp. 50-85.
24 T. Ikai, C. Yamamoto, M. Kamigaito and Y. Okamoto, *Chem. Lett.*, 2006, **35**, 1250-1251.
25 G. R. Zhu, H. Zhong, Q. H. Yang and C. Li, *Microporous Mesoporous Mat.*, 2008, **116**, 36-43.
26 S. Liu, R. Deng, W. Li and J. Zhu, *Adv. Funct. Mater.*, **22**, 1541-1541.
27 C. A. Mitchell, J. L. Bahr, S. Arepalli, J. M. Tour and R. Krishnamoorti, *Macromolecules*, 2002, **35**, 8825-8830.
28 S. Safran, P. Pincus and D. Andelman, *Science*, 1990, **248**, 354-356.
29 H. W. Oviatt, Jr., K. J. Shea and J. H. Small, *Chem. Mater.*, 1993, **5**, 943-950.
30 D. A. Loy, G. M. Jamison, B. M. Baugher, E. M. Russick, R. A. Assink, S. Prabakar and K. J. Shea, *J. Non-Cryst. Solids*, 1995, **186**, 44-53.
31 D. A. Loy, K. A. Obrey-DeFriend, K. V. Wilson Jr, M. Minke, B. M. Baugher, C. R. Baugher, D. A. Schneider, G. M. Jamison and K. J. Shea, *J. Non-Cryst. Solids*, 2013, **362**, 82-94.
32 L. L. Hench and J. K. West, *Chem. Rev.*, 1990, **90**, 33-72.
33 B. Sébille, N. Thuaud, J. Piquion and N. Behar, *J. Chromatogr. A*, 1987, **409**, 61-69.
34 R. Y. Sheinfain, O. Stas and I. Neimark, *Kolloidn. Zh*, 1965, **27**, 916-920.
35 K. Sing, *Pure Appl. Chem.* 1982, **54**, 2201-2218.
36 J. C. Groen, L. A. A. Peffer and J. Pérez-Ramírez, *Microporous Mesoporous Mat.*, 2003, **60**, 1-17.

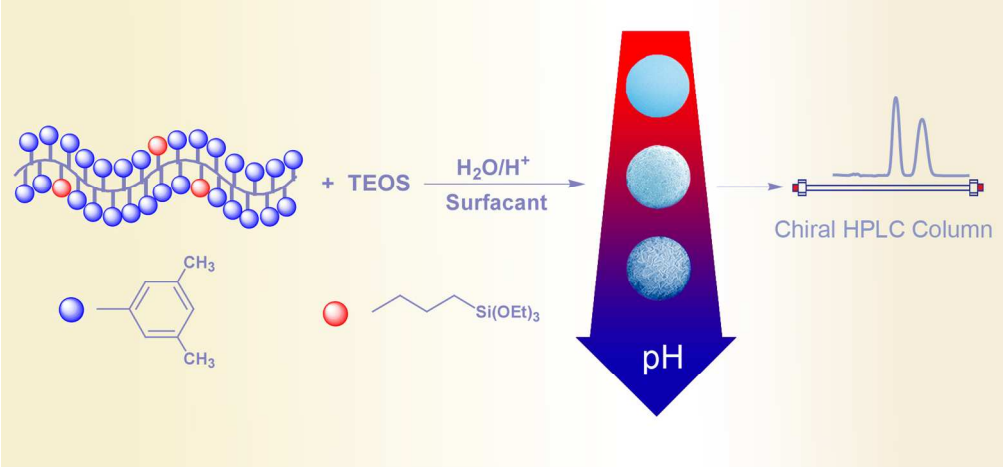

150x70mm (300 x 300 DPI)